ACADEMIC PRESS

Available online at www.sciencedirect.com
SCIENCE DIRECT®

Journal of Solid State Chemistry 173 (2003) 244–250

JOURNAL OF SOLID STATE CHEMISTRY

http://elsevier.com/locate/jssc

Synthesis, structure and magnetic properties of the new mixed-valence vanadate $Na_2SrV_3O_9$

R.V. Shpanchenko,[a,*] V.V. Chernaya,[a] E.V. Antipov,[a] J. Hadermann,[b] E.E. Kaul,[c] and C. Geibel[c]

[a] *Department of Chemistry, Moscow State University, 119899 Moscow, Russia*
[b] *EMAT University of Antwerp (RUCA), Groenenborgerlaan 171, 2020 Antwerp, Belgium*
[c] *MPI CPfS Nöthnitzer Street 40, 01187 Dresden, Germany*

Received 26 April 2002; received in revised form 6 December 2002; accepted 15 December 2002

Abstract

The new complex oxide $Na_2SrV_3O_9$ was synthesized and investigated by means of X-ray diffraction, electron microscopy and magnetic susceptibility measurements. This oxide has a monoclinic unit cell with parameters $a = 5.416(1)$ Å, $b = 15.040(3)$ Å, $c = 10.051(2)$ Å, $\beta = 97.03(3)^\circ$, space group $P2_1/c$ and $Z = 4$. The crystal structure of $Na_2SrV_3O_9$, as determined from X-ray single-crystal data, is built up from isolated chains formed by square $V^{4+}O_5$ pyramids. Neighboring pyramids are linked by two bridging $V^{5+}O_4$ tetrahedra sharing a corner with each pyramid. The Na and Sr atoms are situated between the chains. Electron diffraction and HREM investigations confirmed the crystal structure. The temperature dependence of the susceptibility indicates low-dimensional magnetic behavior with a sizeable strength of the magnetic intra-chain exchange J of the order of 80 K, which is very likely due to superexchange through the two VO_4 tetrahedra linking the magnetic V^{4+} cations.

Keywords: Sodium strontium vanadium oxide; Low-dimensional magnetic system

1. Introduction

Complex vanadium oxides with a low oxidation state of vanadium have attracted the attention of researchers due to their interesting magnetic properties. Many new compounds were discovered in binary and ternary systems. Most of the structures having magnetic V^{4+} cations form low-dimensional magnetic systems, either one- or two-dimensional [1]. When the average oxidation state of the vanadium atoms is in the range $+4 < V_V < +5$, the type of resulting structure will depend on the coordination arrangement of the vanadium atoms. Thus, if the coordination polyhedra are only square pyramids, layered or pipe-like structures are formed [2]. If several types of vanadium coordination polyhedra are present, different possibilities for structure construction exist.

In the framework of our research, we consider only "one-dimensional" structures containing chains where every polyhedron with a magnetic V^{4+} cation is linked only with two neighboring polyhedra-containing V^{4+}. The recently reported compounds with common formulae $A_2V_3O_9$ (A = Sr, Pb, Ba) [3–7] have structures consisting of chains of $V^{4+}O_6$ octahedra. In the Sr- and Pb-based compounds, the octahedra are connected via common corners to form chains, which are linked by $V^{5+}O_4$ tetrahedra into layers. In the Ba-based compound, octahedra linked by common edges form rutile-like chains, which are not linked with each other. The $V^{+5}O_4$ tetrahedra are connected to the octahedra by corner sharing.

Replacement of V^{5+} by P^{5+} or As^{5+} often results in the formation of compounds having similar compositions which can be expressed as $A_2(VO)(XO_4)_2$ (X= V, P, As; A = Sr, Ba) [8,9]. In some cases, this replacement leads to the same (or similar) structure types. Thus, $Sr_2(VO)(XO_4)_2$ (X= P, As) structures are essentially the same as $Sr_2V_3O_9$ [3]. In other cases, the replacement of V^{5+} by P^{5+} leads to a profound change of the structure.

*Corresponding author. Fax: +7-095-939-4788.
E-mail address: shpanchenko@icr.chem.msu.ru (R.V. Shpanchenko).

0022-4596/03/$ - see front matter
doi:10.1016/S0022-4596(03)00039-2

For example, the $Ba_2(VO)(PO_4)_2$ structure shows isolated square pyramids linked by two tetrahedra instead of the rutile-like chains of octahedra in the $Ba_2V_3O_9$ structure. Similar structures with chains of octahedra are observed in the $A(VO)_2(PO_4)_2$ (A= Ca, Ba) vanadyl phosphates [10,11]. Some of the vanadium oxides with organic cations contain in their structures zigzag chains of edge-shared octahedra, such chains being linked by tetrahedrally coordinated V^{5+} [2].

One may suggest that the presence, in the same structure, of two types of A cations with different charge should lead to their ordering and consequently to the formation of new structures. Starting from the $Sr_2V_3O_9$ structure, we tried to synthesize a new compound by exchanging one Sr^{2+} cation by two Na^+. Since the parent structure has not enough interstices to accommodate the extra sodium ions, we expected some structural transformations but with the preservation of the "low-dimensional" nature of the structure. We indeed obtained a new compound crystallizing in a new one-dimensional structure.

Here, we present the results of the synthesis and the investigation of the new complex oxide $Na_2SrV_3O_9$ using X-ray diffraction, electron diffraction (ED) and HREM techniques as well as magnetic susceptibility measurements.

2. Experimental

Single-phase samples of the new compound $Na_2SrV_3O_9$ were obtained by annealing a stoichiometric mixture of $Sr_2V_2O_7$, $Na_4V_2O_7$ and VO_2 in a sealed and evacuated silica tube at 650°C for 7 days with intermediate regrinding. $Sr_2V_2O_7$ was synthesized from $SrCO_3$ and V_2O_5 by annealing at 700°C for 24 h in air. $Na_4V_2O_7$ was obtained from Na_2CO_3 and V_2O_5 by heating at 650°C for 4 days in air followed by drying under vacuum at 400°C. All subsequent operations with highly hygroscopic $Na_4V_2O_7$ were carried out in a glove box under argon atmosphere.

The isostructural complex oxide $Na_2CaV_3O_9$ was obtained by melting a stoichiometric mixture of $Ca_2V_2O_7$, Na_2CO_3, VO_2 and V_2O_5 in dynamic vacuum ($\approx 10^{-6}$ atm) at 850°C. However, the use of different synthetic techniques always resulted in multiphase mixtures. The powder X-ray pattern of the new $Na_2CaV_3O_9$ compound was indexed in monoclinic symmetry with lattice parameters $a = 5.3818(15)$ Å, $b = 14.628(9)$ Å, $c = 9.842(3)$ Å, $\beta = 96.25(3)°$, and $Z = 4$ which are significantly smaller than those for Sr-containing compound due to the difference in the Ca and Sr atomic radii. Since we could not obtain pure samples of this compound, we did not investigate its structural and physical properties.

Table 1
Measurement conditions and structural parameters of $Na_2SrV_3O_9$

Space group	$P2_1/c$ (no. 14)
a (Å)	5.416(1)
b (Å)	15.040(3)
c (Å)	10.051(2)
β (°)	97.03(3)
Z	4
Cell volume (Å^3)	812.6(5)
Calculated density (g cm^{-3})	3.518
μ (cm^{-1})	105.13
Crystal size (mm)	$0.02 \times 0.05 \times 0.1$
No. of measured reflections	1491
No. of unique reflections ($F > 2\sigma(F)$)	1423
R_{eq}	0.035
No. of reflections in refinement ($F > 4\sigma(F)$)	924
Weighing scheme	Unit
Number of atom sites	15
No. of variables	91
2θ (max) and $\sin\theta/\lambda$ (max)	49.94, 0.594
R_F, R_{wF}	0.045, 0.045

Light-brown single crystals of $Na_2SrV_3O_9$ for structure refinement were obtained by melting a stoichiometric mixture of $SrCO_3$, $NaVO_3$ and VO_2 in dynamic vacuum at 730°C. Single-crystal X-ray diffraction data were collected on a CAD-4 diffractometer. The measurement conditions and the structural parameters of $Na_2SrV_3O_9$ are listed in Table 1. An empirical absorption correction was applied using the ψ-scan method and reflections with $F > 4\sigma(F)$ were used for the structure refinement. All computations were carried out using the CSD program package [12]. The heavy atom coordinates were taken from the results of the direct method solution. The positions of the vanadium and oxygen atoms were found using a Fourier and difference Fourier synthesis sequence. The anisotropic thermal parameters were refined only for the cations due to insufficient number of experimental intensities. The final residuals are $R_F = 0.045$ and $R_w = 0.045$.

ED and high-resolution electron microscopy (HREM) were performed with a JEOL 4000EX microscope. The image simulations were made using the MacTempas software.

Magnetic susceptibility measurements were performed in the temperature range 2–400 K and in applied magnetic fields between 0.05 and 7 T with a Quantum Design MPMS SQUID magnetometer.

3. Results and discussion

The overall view of the $Na_2SrV_3O_9$ crystal structure along the a direction is shown in Fig. 1. $V^{4+}O_5$ pyramids linked by four $V^{5+}O_4$ tetrahedra with neighboring pyramids form chains along the a direction. The chains are not connected with each other and form layers parallel to the $a-b$ plane. The strontium and

sodium atoms are situated in an ordered manner in the interstices between these layers. The pyramids are slightly distorted. The apical O(4) oxygen atom in the pyramids has a short (1.606 Å) distance to V(1) which corresponds to a double bonding in a vanadyl group. Two opposite pairs of oxygen atoms are connected with $V(2)O_4$ and $V(3)O_4$ tetrahedra. Two pairs of V–O bond-lengths (about 1.66 and 1.76 Å) exist in the tetrahedra. The tetrahedra are not equivalent due to the ordering of Na and Sr atoms situated between the layers. The vanadyl bonds inside the pyramids are oriented in the same direction within one chain, but in opposite direction in neighboring chains. The Na atoms are situated in front of the apical vertex of the pyramids and the Sr atoms are in front of their square basis. The bond valence sums calculated for cations (Table 2) confirm their oxidation states.

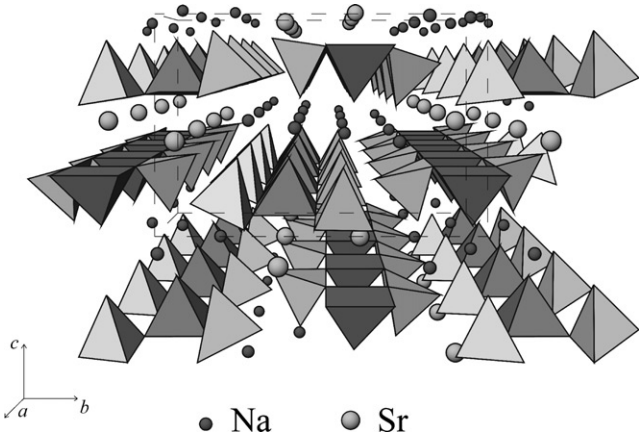

Fig. 1. Overall view of the $Na_2SrV_3O_9$ crystal structure projected along the *a*-axis.

The Na(1) atoms have a slightly distorted octahedral arrangement, whereas the coordination polyhedra for the Na(2) atoms are strongly distorted octahedra due to a tilt of the apical O(5) atom (Fig. 2). The Sr atom is situated in a 10-vertex polyhedra. The coordination polyhedra for the sodium and strontium atoms are shown in Fig. 2. The atomic coordinates and main interatomic distances and angles in the $Na_2SrV_3O_9$ structure are listed in Tables 2 and 3, respectively.

There are many known structures of vanadium compounds in a low oxidation state between +4 and +5, where a three-dimensional or layered framework is constructed by different combinations of tetrahedra and square pyramids. However, the $Na_2SrV_3O_9$ structure is the first example where isolated chains consisting of $V^{4+}O_5$ pyramids linked only by $V^{5+}O_4$ tetrahedra exist. A similar structure was described by Wadewitz and Müller-Buschbaum [9] for $Ba_2(VO)(PO_4)_2$ vanadyl phosphate. In Fig. 3, we compare the chains in the crystal structures of (a) $Na_2SrV_3O_9$ and (b) $Ba_2(VO)(PO_4)_2$. The large size of the interstices occupied by

Table 2
Positional and thermal parameters for $Na_2SrV_3O_9$

Atom	Wyck. posit.	*x/a*	*y/b*	*z/c*	B_{eq} (Å^2)[a]	Valence from BVS
Sr	4*e*	0.2561(2)	0.61247(8)	0.0300(1)	0.71(3)	1.97
Na(1)	4*e*	0.247(1)	0.5677(4)	0.4768(6)	1.9(1)	1.09
Na(2)	4*e*	0.759(1)	0.7899(3)	0.9686(5)	1.4(1)	1.11
V(1)	4*e*	0.2896(4)	0.4010(1)	0.2143(2)	0.51(4)	4.19
V(2)	4*e*	0.2132(4)	0.4524(1)	0.7957(2)	0.51(4)	5.10
V(3)	4*e*	0.2163(4)	0.7370(1)	0.7552(2)	0.54(5)	5.16
O(1)	4*e*	0.483(2)	0.5143(5)	0.8510(8)	0.7(1)	
O(2)	4*e*	0.197(2)	0.7825(6)	0.0912(9)	1.0(2)	
O(3)	4*e*	0.031(2)	0.4853(6)	0.1480(8)	0.9(1)	
O(4)	4*e*	0.342(2)	0.4095(6)	0.3748(9)	1.2(2)	
O(5)	4*e*	0.483(2)	0.6869(5)	0.8420(8)	0.7(1)	
O(6)	4*e*	0.182(2)	0.4394(6)	0.6310(9)	1.6(2)	
O(7)	4*e*	0.254(2)	0.6545(6)	0.2790(8)	0.8(2)	
O(8)	4*e*	0.752(2)	0.6402(6)	0.1128(8)	1.1(2)	
O(9)	4*e*	0.965(2)	0.6908(6)	0.8283(9)	1.0(2)	

Anisotropic thermal parameters[b]

Atom	B11	B22	B33	B12	B13	B23
Sr1	0.76(4)	0.66(5)	0.70(4)	−0.00(4)	0.08(3)	0.07(4)
Na1	1.6(2)	1.7(2)	2.1(2)	−0.1(2)	−0.2(2)	0.3(2)
Na2	1.7(2)	0.7(2)	1.8(2)	0.1(2)	−0.0(2)	−0.6(2)
V1	0.38(7)	0.56(8)	0.58(8)	−0.12(7)	0.09(6)	−0.01(7)
V2	0.34(8)	0.59(8)	0.70(8)	0.02(6)	0.12(6)	0.05(7)
V3	0.52(8)	0.52(8)	0.75(8)	−0.14(6)	0.11(6)	0.11(7)

[a] $B_{eq}=1/3[B11a^{*2}a^2+\cdots+2B23b^*c^*bc\cos\alpha]$.
[b] $T=\exp[-1/4(B11a^{*2}h^2+\cdots+2B23b^*c^*k\,l)]$.

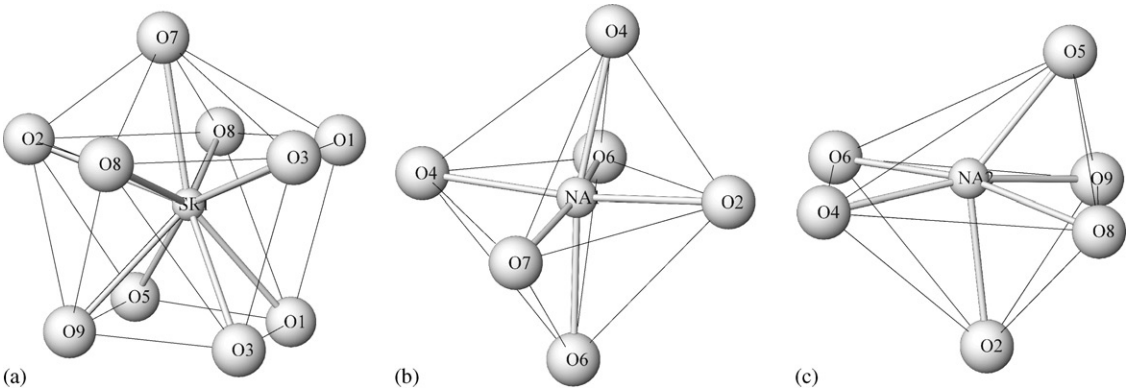

Fig. 2. Coordination polyhedra for the Sr atoms (a) and for the Na(1) and Na(2) atoms ((b) and (c) respectively).

Table 3
Main interatomic distances (Å) and angles (°) in the $Na_2SrV_3O_9$ structure

Sr–O(1)	2.581(9)	Na(1)–O(7)	2.38(1)	V(1)–O(4)	1.606(9)
Sr–O(7)	2.581(9)	Na(1)–O(6)	2.44(1)	V(1)–O(5)	1.939(9)
Sr–O(5)	2.627(9)	Na(1)–O(6)	2.53(1)	V(1)–O(1)	1.942(9)
Sr–O(3)	2.630(9)	Na(1)–O(4)	2.55(1)	V(1)–O(3)	1.944(9)
Sr–O(2)	2.660(9)	Na(1)–O(2)	2.56(1)	V(1)–O(9)	1.964(9)
Sr–O(3)	2.664(9)	Na(1)–O(4)	2.67(1)	V(2)–O(6)	1.66(1)
Sr–O(9)	2.682(9)	Na(2)–O(5)	2.41(1)	V(2)–O(8)	1.669(9)
Sr–O(1)	2.731(9)	Na(2)–O(9)	2.42(1)	V(2)–O(1)	1.762(9)
Sr–O(8)	2.746(9)	Na(2)–O(6)	2.50(1)	V(2)–O(3)	1.771(9)
Sr–O(8)	2.977(9)	Na(2)–O(4)	2.50(1)	V(3)–O(7)	1.655(9)
		Na(2)–O(2)	2.54(1)	V(3)–O(2)	1.667(9)
		Na(2)–O(8)	2.68(1)	V(3)–O(5)	1.761(9)
				V(3)–O(9)	1.764(9)
O(4)–V(1)–O(1)	104.1(4)	O(1)–V(2)–O(6)	110.9(5)	O(2)–V(3)–O(7)	107.9(5)
O(4)–V(1)–O(5)	107.8(4)	O(3)–V(2)–O(6)	113.2(5)	O(5)–V(3)–O(7)	105.6(4)
O(4)–V(1)–O(3)	108.9(4)	O(6)–V(2)–O(8)	116.4(5)	O(7)–V(3)–O(9)	114.5(4)
O(4)–V(1)–O(9)	108.0(4)	O(1)–V(2)–O(3)	103.9(4)	O(2)–V(3)–O(5)	111.3(4)
O(1)–V(1)–O(9)	147.8(4)	O(1)–V(2)–O(8)	103.7(4)	O(2)–V(3)–O(9)	112.7(5)
O(3)–V(1)–O(5)	143.3(4)	O(3)–V(2)–O(8)	107.7(4)	O(5)–V(3)–O(9)	104.6(4)
O(5)–V(1)–O(9)	84.9(4)	V(1)–O(1)–V(2)	140.8(5)	V(1)–O(1)–V(3)	131.2(5)
O(1)–V(1)–O(3)	85.4(4)	V(1)–O(1)–V(2)	140.8(5)	V(1)–O(1)–V(3)	137.9(5)

Ba^{2+} cations and the substitution of Ba^{2+} cations by the smaller Sr^{2+} allows the accommodation of extra A cations in the structure. At the same time, the size of the interstices occupied by the A cations increased due to the rotation of the vanadyl oxygen of every second pyramid to opposite directions. So, all pyramids in the chains of the $Na_2SrV_3O_9$ structure are turned to the same direction. The ordered placement of Sr^{2+} and Na^{+} results in the alignment of the chains which form layers in the $Na_2SrV_3O_9$ structure. A further similar structure was found for $Ba_2(VO)(PO_4)_2 \cdot H_2O$ [13]. However, in the latter case the presence of an extra oxygen from the H_2O molecule transforms the VO_5 pyramids into VO_6 octahedra. The vanadium atoms in the octahedra statistically occupy positions above and below the equatorial plane as it is often observed in structures with octahedrally coordinated V^{4+} cations.

The ED patterns (Fig. 4) can be indexed using the cell parameters obtained from X-ray diffraction. The $[010]^*$ zone shows the extinction condition $h\,0\,l{:}l = 2n$. The $[100]^*$ and $[001]^*$ appear to show no extinctions, yet by tilting away from the perfect orientation the reflections $0\,k\,0{:}k \neq 2n$ and $0\,l\,0{:}l \neq 2n$ disappear, indicating that these are due to double diffraction. Thus the additional extinction conditions $0\,k\,0{:}k = 2n$ and $0\,0\,l{:}l = 2n$ are revealed. These extinction conditions are in agreement with the space group $P2_1/c$.

Fig. 5 shows an HREM image along the [100] direction. The black rectangle outlines the image simulation which was made using the structure model and coordinates proposed above. The simulated image was obtained at a defocus value $\Delta f = -40$ nm and thickness $t = 5$ nm. The projected positions of the atom columns are shown on the white background in the

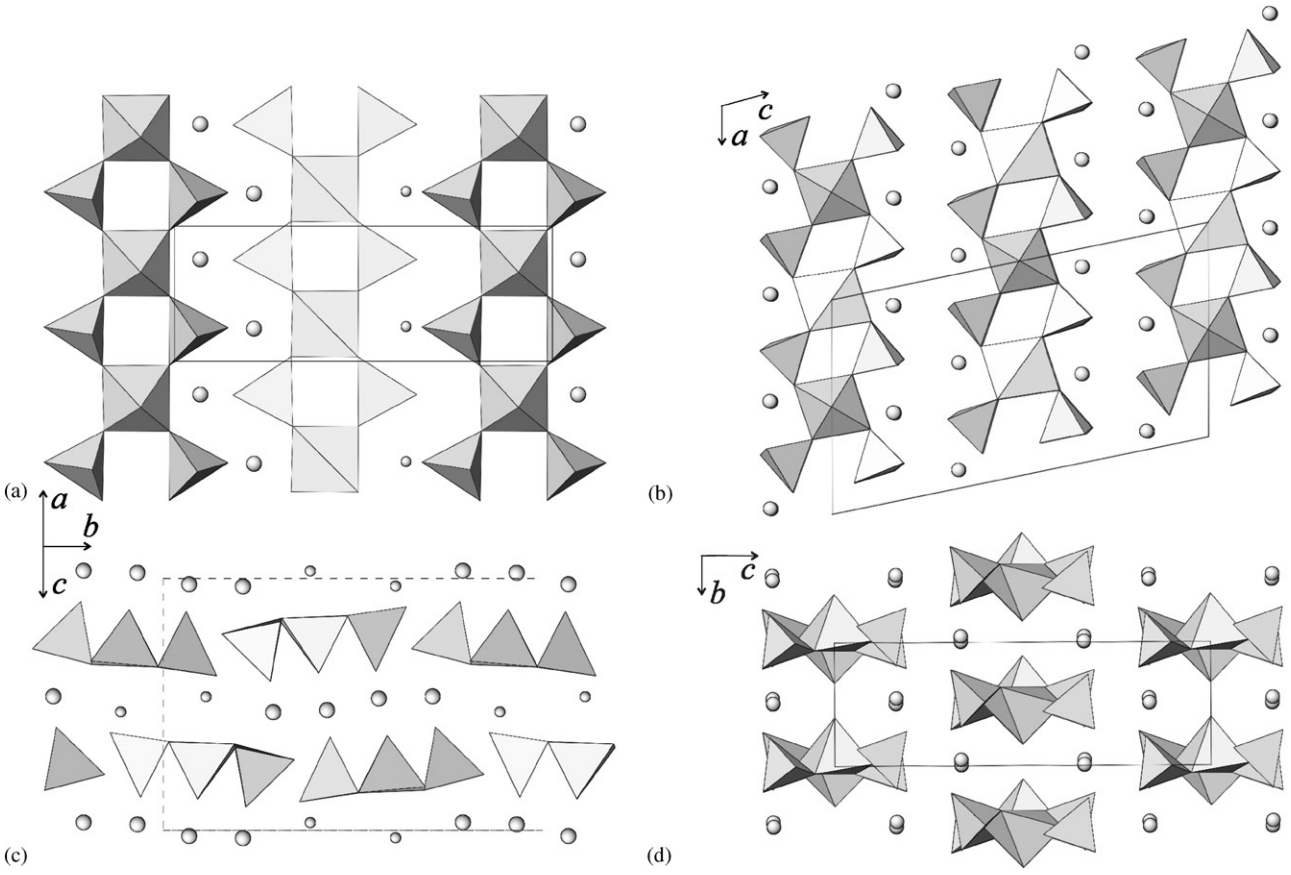

Fig. 3. Crystal structure of $Na_2SrV_3O_9$ ((a) and (c)) and $Ba_2(VO)(PO_4)_2$ ((b) and (d)).

simulation: V as large black dots, Sr as the smaller black dots and Na in gray. The material is very sensitive to the intense electron beam used for high-resolution images and decomposes after a few seconds.

Preliminary susceptibility measurements were performed between 2 and 400 K in fields between 0.05 and 7 T on small polycrystalline samples. The results were affected by a small ferromagnetic impurity contribution, which was independent of the temperature below 400 K. We therefore show in Fig. 6 the temperature dependence of the susceptibility after subtraction of this ferromagnetic contribution. Above 150 K, $\chi(T)$ follows a Curie–Weiss (CW) law with an effective moment of 1.82 μ_B, close to the value of 1.73 μ_B expected for one V^{4+} ion per formula unit, and a CW temperature $\theta = -78$ K. This θ value indicates a significant antiferromagnetic interaction, which is somewhat surprising, since there are no direct V^{4+}–O–V^{4+} superexchange paths in this structure. The most probable exchange is a V–O–O–V–superexchange through each of the two VO_4 tetrahedra (with V^{5+} ions) which connect two V^{4+} pyramids along the V^{4+} chain. Although such exchange paths are generally neglected, a comparable strength of a magnetic exchange through PO_4 tetrahedra was proved in recent investigations of the compound $(VO)_2P_2O_7$ [14–16]. $Sr_2NaV_3O_9$ is thus a further simple example that complex exchange paths can lead to a quite strong magnetic exchange and have to be considered when discussing magnetic interactions in such compounds. Below 150 K, the increase of $\chi(T)$ with decreasing temperature is weaker than expected for a CW law, pointing to low-dimensional magnetic correlations. It is presently not clear whether the increase of the susceptibility at even lower temperatures, below 25 K is an extrinsic contribution due to defects or whether it is an intrinsic contribution due to the effect of the Dzyaloshinsky–Moriya interaction [17]. We found no evidence for long-range magnetic order above 2 K.

In summary, we have synthesized a new complex vanadium oxide, $Na_2SrV_3O_9$, and determined its structure and its magnetic properties. The structure of $Na_2SrV_3O_9$ is built up from isolated chains formed by square $V^{4+}O_5$ pyramids linked by two bridging $V^{5+}O_4$ tetrahedra. The chains are arranged in layers separated by Sr and Na. Susceptibility measurements indicate a low-dimensional behavior with a sizeable magnetic exchange between the V^{4+} along the chain, which is mediated by the connecting $V^{5+}O_4$ tetrahedra.

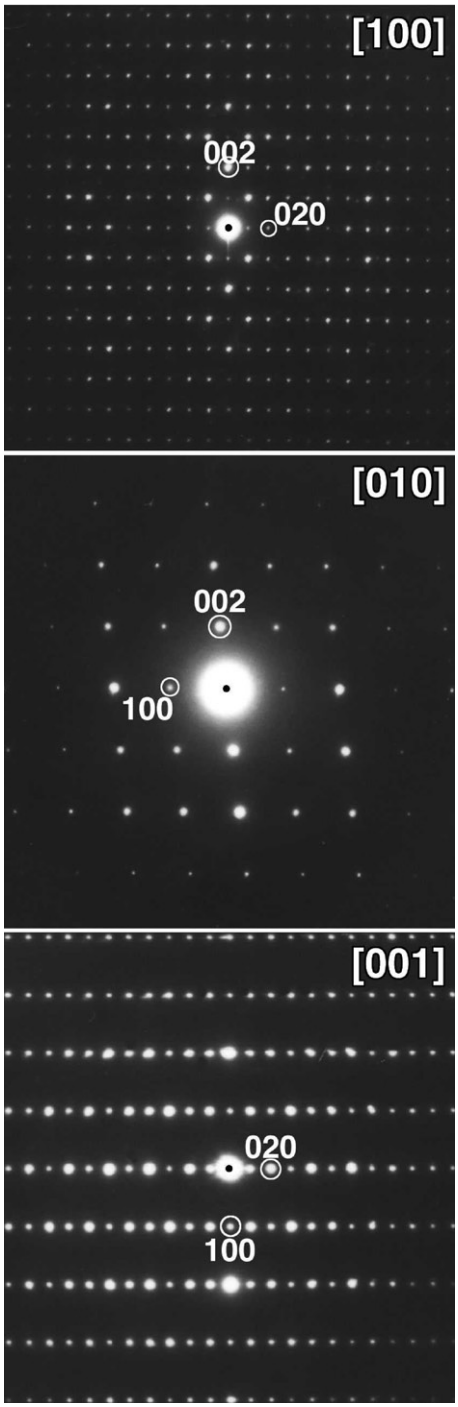

Fig. 4. ED patterns of the [100]*, [010]*and [001]* zones for $Na_2SrV_3O_9$.

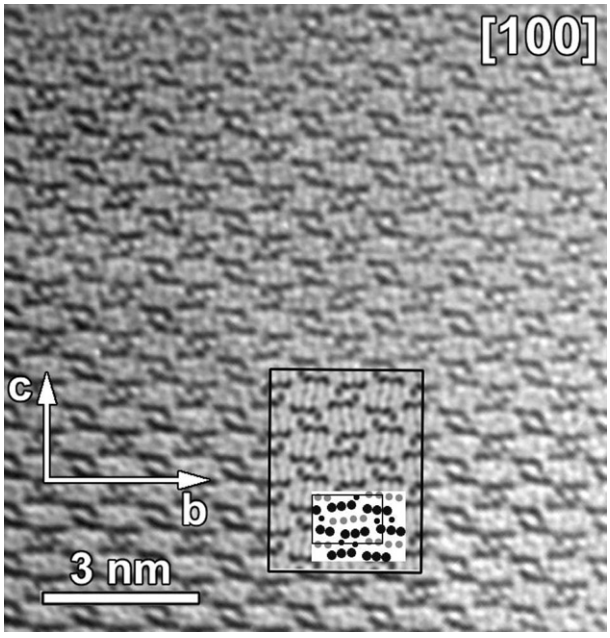

Fig. 5. HREM image of $Na_2SrV_3O_9$ taken along the [100] direction. The image simulation based on proposed model is shown as an inset, separated from the image by a black border.

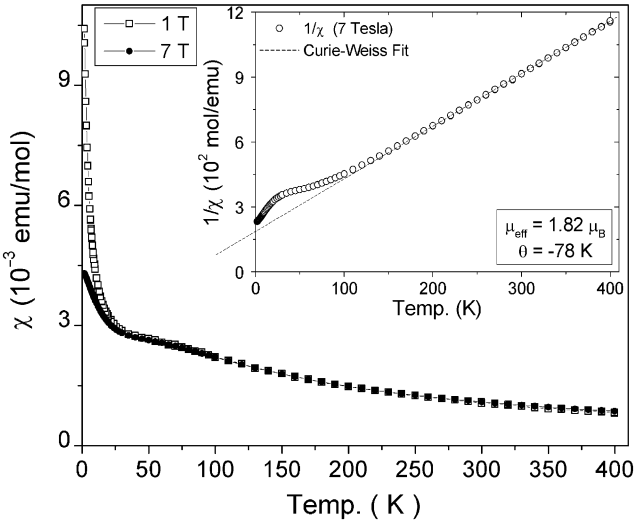

Fig. 6. Magnetic susceptibility of $Na_2SrV_3O_9$ vs. temperature in fields of 1 and 7 T.

Acknowledgments

The authors are grateful to NATO for financial support (Grant PST.CLG.976956). R.Sh. and V.Ch. gratefully acknowledge MPI CPfS for their stay in Dresden. Part of this work has been performed within the framework of IUAP4/10.

References

[1] Y. Ueda, Chem. Mater. 10 (1998) 265–2664.
[2] P.Y. Zavalij, M.S. Whittingham, Acta Crystallogr. B 55 (1999) 627–663.
[3] J. Feldmann, Hk. Müller-Buschbaum, Z. Naturforsch. B 50 (1995) 43–46.
[4] J. Feldmann, Hk. Müller-Buschbaum, Z. Naturforsch. B 51 (1996) 489–492.
[5] A.-C. Dhaussy, F. Abraham, O. Mentré, H. Stainfink, J. Solid State Chem. 126 (1996) 328–335.
[6] O. Mentré, A.-C. Dhaussy, F. Abraham, H. Stainfink, J. Solid State Chem. 140 (1998) 417–427.

[7] O. Mentré, A.C. Dhaussy, F. Abraham, E. Suard, H. Stainfink, Chem. Mater. 11 (1999) 2408–2416.
[8] C. Wadewitz, Hk. Müller-Buschbaum, Z. Naturforsch. B 51 (1996) 489–492.
[9] C. Wadewitz, Hk. Müller-Buschbaum, Z. Naturforsch. B 51 (1996) 1290–1294.
[10] K.H. Lii, B.R. Chueh, H.Y. Kang, S.L. Wang, J. Solid State Chem. 99 (1992) 72–77.
[11] A. Grandin, J. Chardon, M.M. Borel, A. Leclaire, B. Raveau, J. Solid State Chem. 99 (1992) 297–302.
[12] L.G. Akselrud, P.Yu. Zavalii, Yu.N. Grin, V.K. Pecharski, B. Baumgartner, E. Wölfel, Mater. Sci. Forum 133–136 (1993) 335–340.
[13] W.T.A. Harrison, S.C. Lim, J.T. Vaughey, A.J. Jacobson, D.P. Goshorn, J.W. Johnson, J. Solid State Chem. 113 (1994) 444–447.
[14] A.W. Garret, S.E. Nagler, D.A. Tennant, B.C. Sales, T. Barnes, Phys. Rev. Lett. 79 (1997) 745–748.
[15] D.A. Tennant, S.E. Nagler, A.W. Garret, T. Barnes, C.C. Toradi, Phys. Rev. Lett. 78 (1997) 4998–5001.
[16] J. Kikuchi, K. Motoya, T. Yamauchi, Y. Ueda, Phys. Rev. B 60 (1999) 6731–6739.
[17] R. Feyerherm, S. Abens, D. Günther, T. Ishida, M. Meißner, M. Meschke, T. Nogami, M. Steiner, J. Phys.: Condens. Matter 12 (2000) 8495–8509.